Supporting Information for "14-year acceleration along the Japan trench and the Sagami trough"

Lou Marill[1], David Marsan[1], Anne Socquet[1], Mathilde Radiguet [1], Nathalie Cotte[1], and Baptiste Rousset[2]

[1]Univ. Grenoble Alpes, Univ. Savoie Mont Blanc, CNRS, IRD, Univ. Gustave Eiffel, ISTerre, 38000 Grenoble, France

[2]Univ. Calif. Berkeley, Dept. Earth & Planetary Sci., Berkeley, CA 94720 USA

Contents of this file

1. Text S1

2. Table S1

3. Figures S1 to S18

Text S1

To describe the transformation of the GPS time series from ITRF2005 to ITRF2014, we detail here the equations controling this transformation. Equation (1) represent the transformation of one point at the Epoch given time (2010.0), all the parameter values are given in Table S1 :

$$\begin{pmatrix} X_{ITRF2005} \\ Y_{ITRF2005} \\ Z_{ITRF2005} \end{pmatrix} = \begin{pmatrix} X_{ITRF2014} \\ Y_{ITRF2014} \\ Z_{ITRF2014} \end{pmatrix} + \begin{pmatrix} T_x \\ T_y \\ T_z \end{pmatrix} + \begin{pmatrix} D & -R_z & R_y \\ R_z & D & -R_x \\ -R_y & R_x & D \end{pmatrix} \begin{pmatrix} X_{ITRF2014} \\ Y_{ITRF2014} \\ Z_{ITRF2014} \end{pmatrix} \quad (1)$$

Equation (2) shows the value of any parameter P at any time t where $\dot{P}$ is the rate of the parameter :

$$P(t) = P(\text{Epoch}) + \dot{P} \times (t - \text{Epoch}) \quad (2)$$

Table S1. Transformation parameters from ITRF2014 to ITRF2005

Solution	T_x (mm)	T_y (mm)	T_z (mm)	D (ppb)	R_x (.001")	R_y (.001")	R_z (.001")	Epoch
Rates	T_x (mm/yr)	T_y (mm/yr)	T_z (mm/yr)	D (ppb/yr)	R_x (.001"/yr)	R_y (.001"/yr)	R_z (.001"/yr)	
ITRF2005	2.6	1.0	-2.3	0.92	0.00	0.00	0.00	2010.0
Rates	0.3	0.0	-0.1	0.03	0.00	0.00	0.00	

From the International Terrestrial Reference Frame website (http://itrf.ensg.ign.fr)

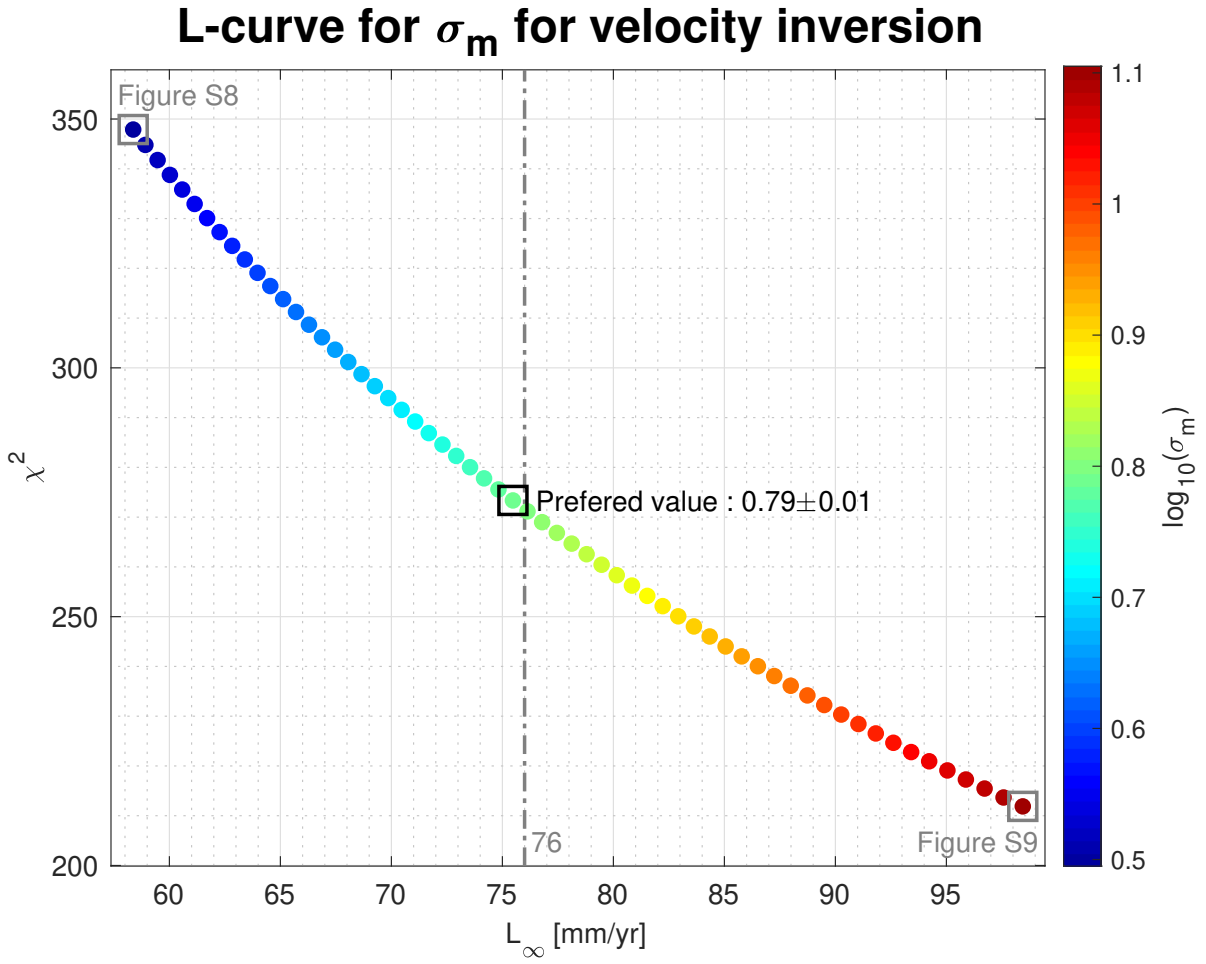

Figure S1. L-curve for σ_m determination for the velocity field inversion. The color correspond to the value of $\log_{10}(\sigma_m)$. Our preferred σ_m value is $10^{0.79}$ ($\log_{10}(\sigma_m) = 0.79$). All the inversion except Figures S8 and S9 are made for $\sigma_m = 10^{0.79}$. Alternative inversions are proposed for $\sigma_m = 10^{0.50}$ (Supplementary Figure S8) and $\sigma_m = 10^{1.10}$ (Supplementary Figure S9).

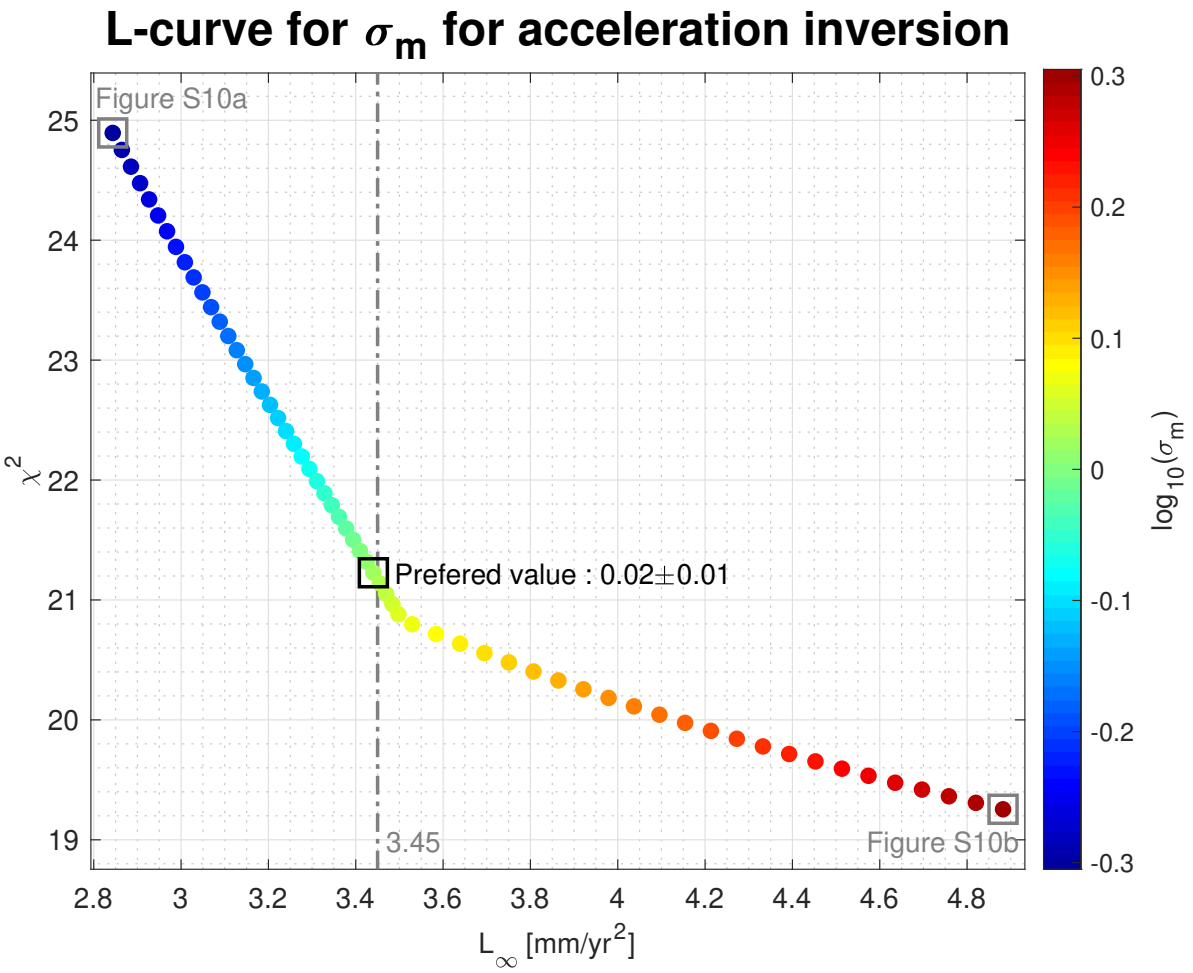

Figure S2. L-curve for σ_m determination for the acceleration field inversion. The color correspond to the value of $\log_{10}(\sigma_m)$. Our preferred σ_m value is $10^{0.02}$ ($\log_{10}(\sigma_m) = 0.02$). All the inversion except Supplementary Figure S10 are made for $\sigma_m = 10^{0.02}$. Alternative inversions are proposed for $\sigma_m = 10^{-0.30}$ (Supplementary Figure S10a) and $\sigma_m = 10^{0.30}$ (Supplementary Figure S10b).

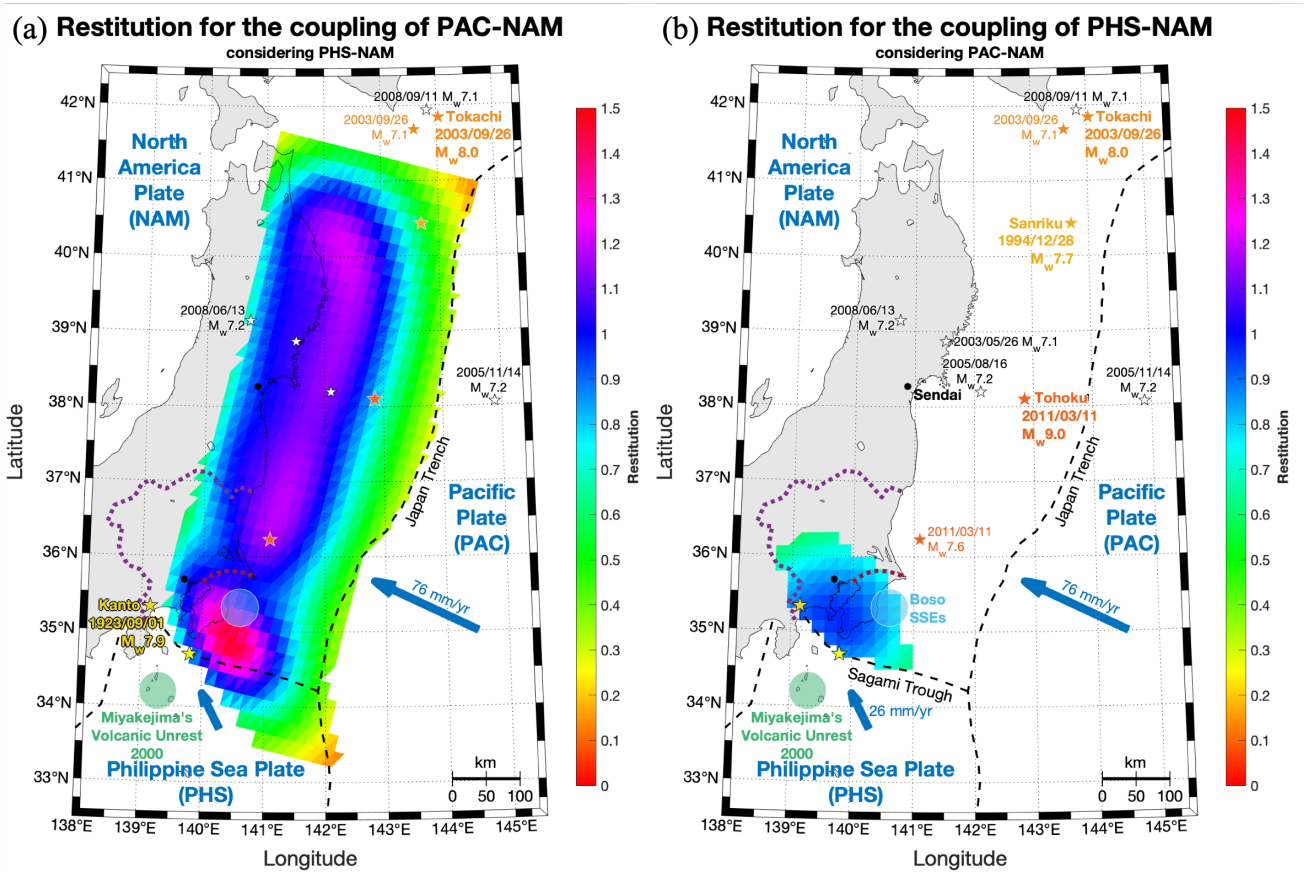

Figure S3. Restitution for the coupling of the Pacific-North America (PAC-NAM) interface (a) and the Philippine Sea-North America (PHS-NAM) interface (b). The color represent the amount of restitution of each sub-fault: 0, the slip is not restored and ∼1, the slip is fully restored. Other elements are described in Figure 1.

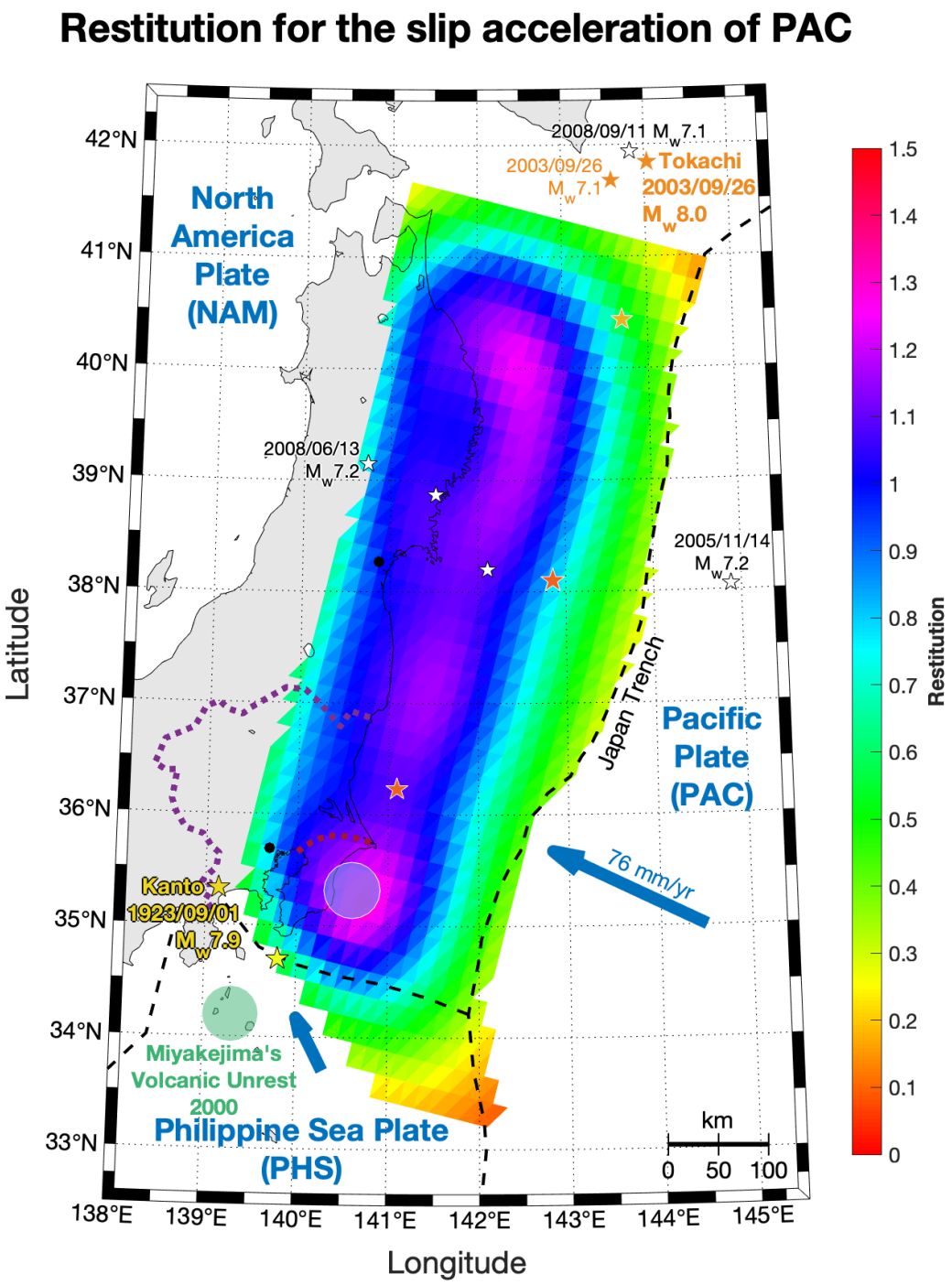

Figure S4. Restitution for the acceleration field inversion of the Pacific (PAC) plate. Same legend than Supplementary Figure S3.

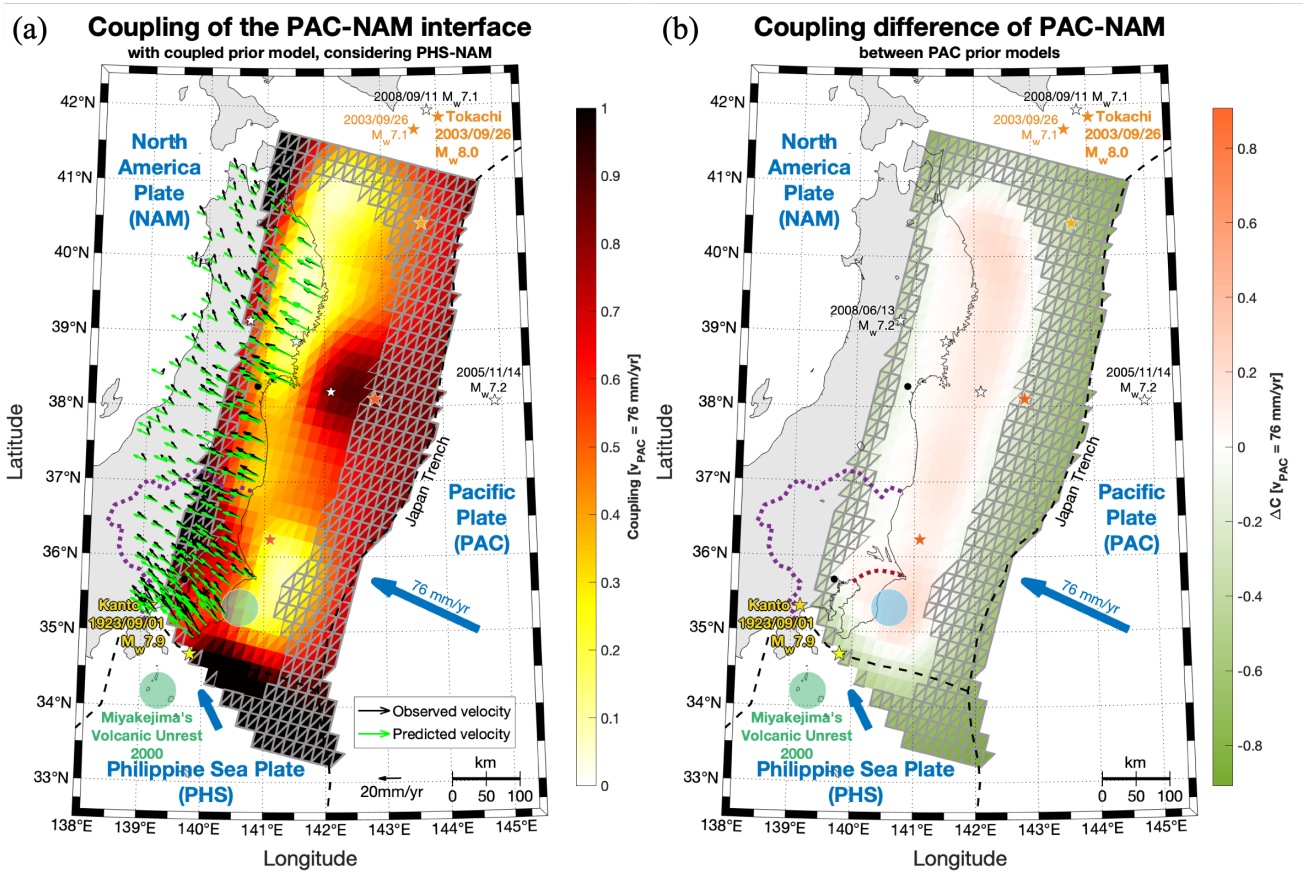

Figure S5. Coupling of the Pacific-North America (PAC-NAM) subduction interface with a fully coupled prior model (a) and the coupling difference between Figure 4a with an uncoupled prior model and (a). (a): Same legend as Figure 4. (b): Orange: sub-fault more coupled for the uncoupled prior model (Figure 4); green: sub-fault less coupled for the uncoupled prior model (Figure 4); other elements are described in Figure 1.

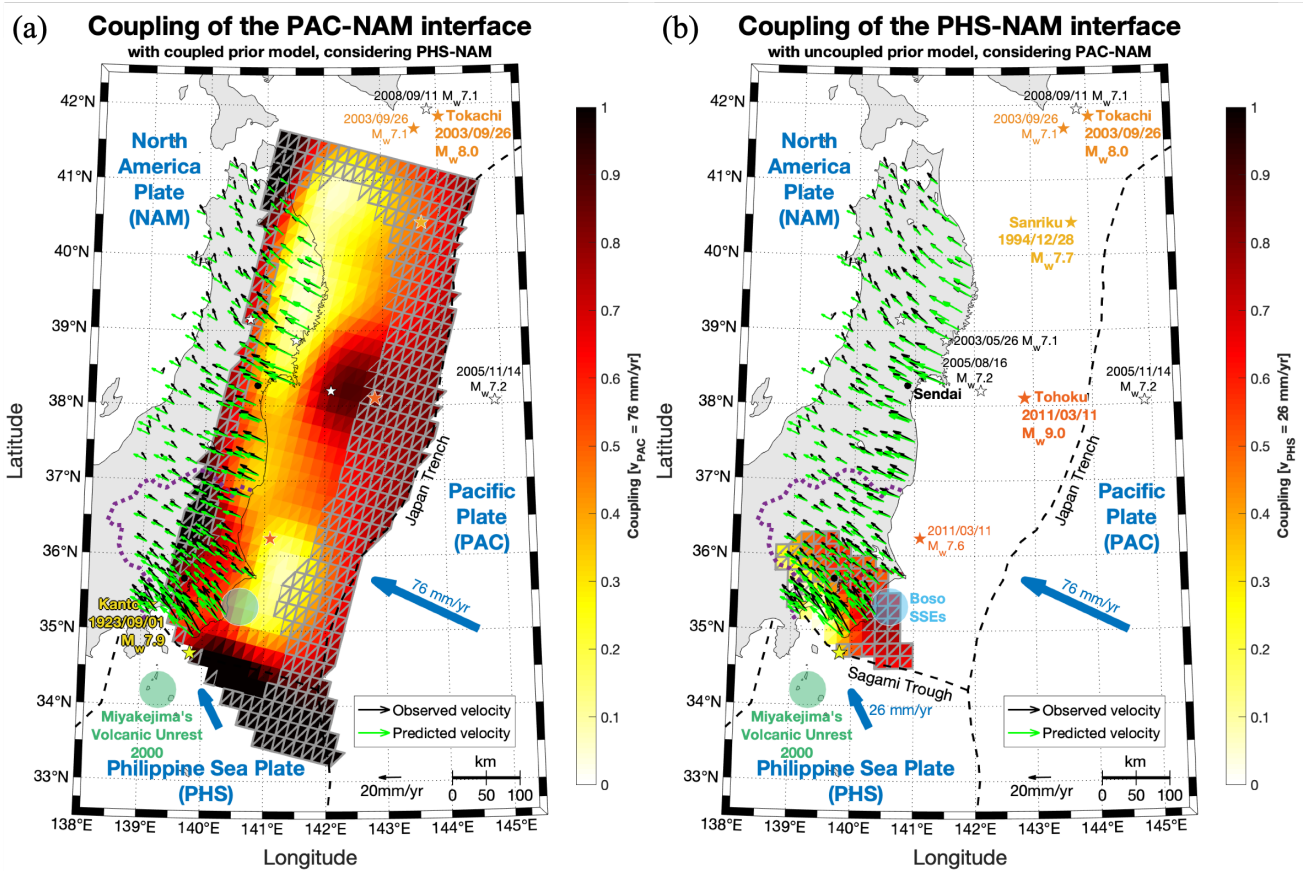

Figure S6. Coupling of the Pacific-North America (PAC-NAM) subduction interface with a fully coupled prior model (a) and coupling of the Philippine Sea-North America (PHS-NAM) subduction interface with a fully uncoupled prior model (b). Same legend as Figure 4.

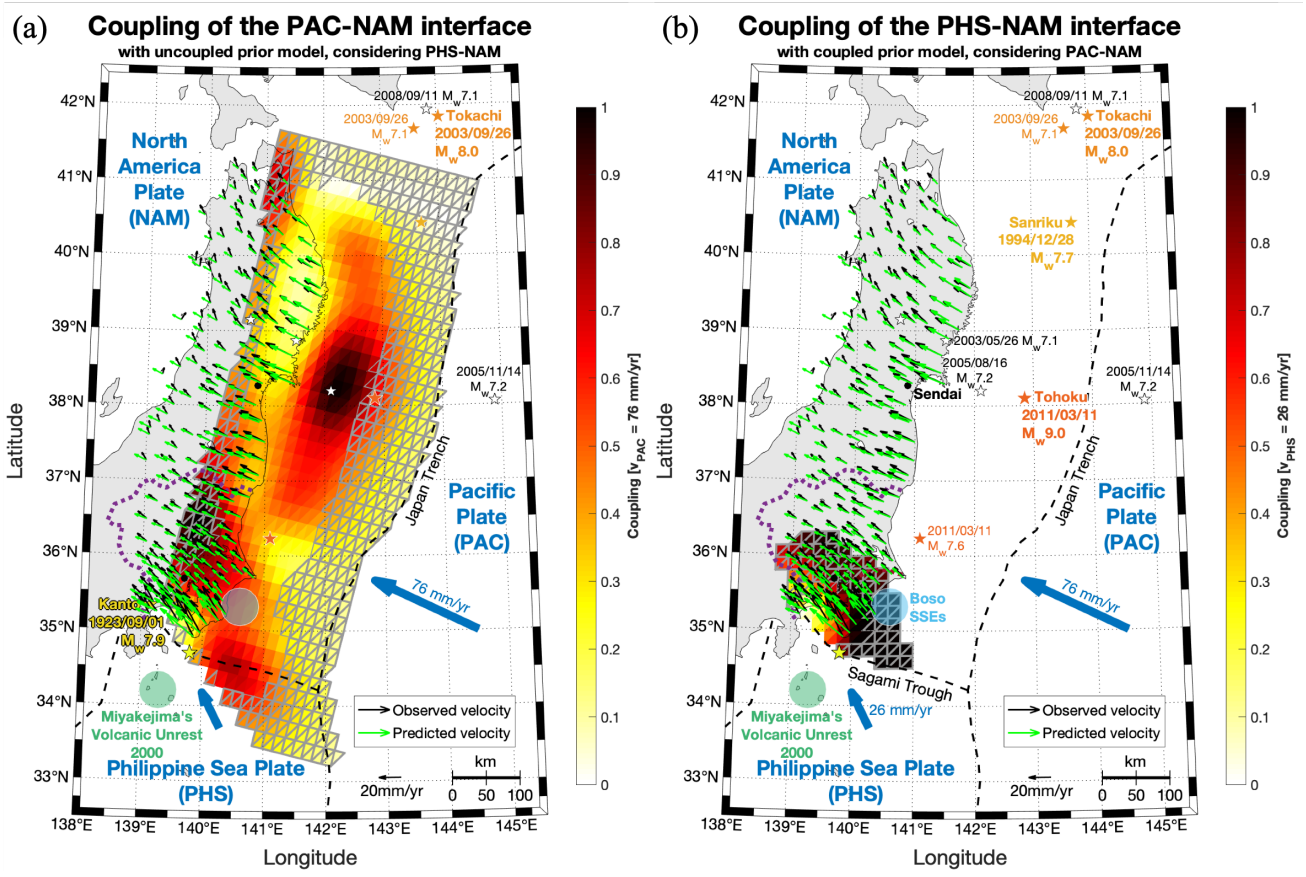

Figure S7. Coupling of the Pacific-North America (PAC-NAM) subduction interface with a fully uncoupled prior model (a) and coupling of the Philippine Sea-North America (PHS-NAM) subduction interface with a fully coupled prior model (b). Same legend as Figure 4.

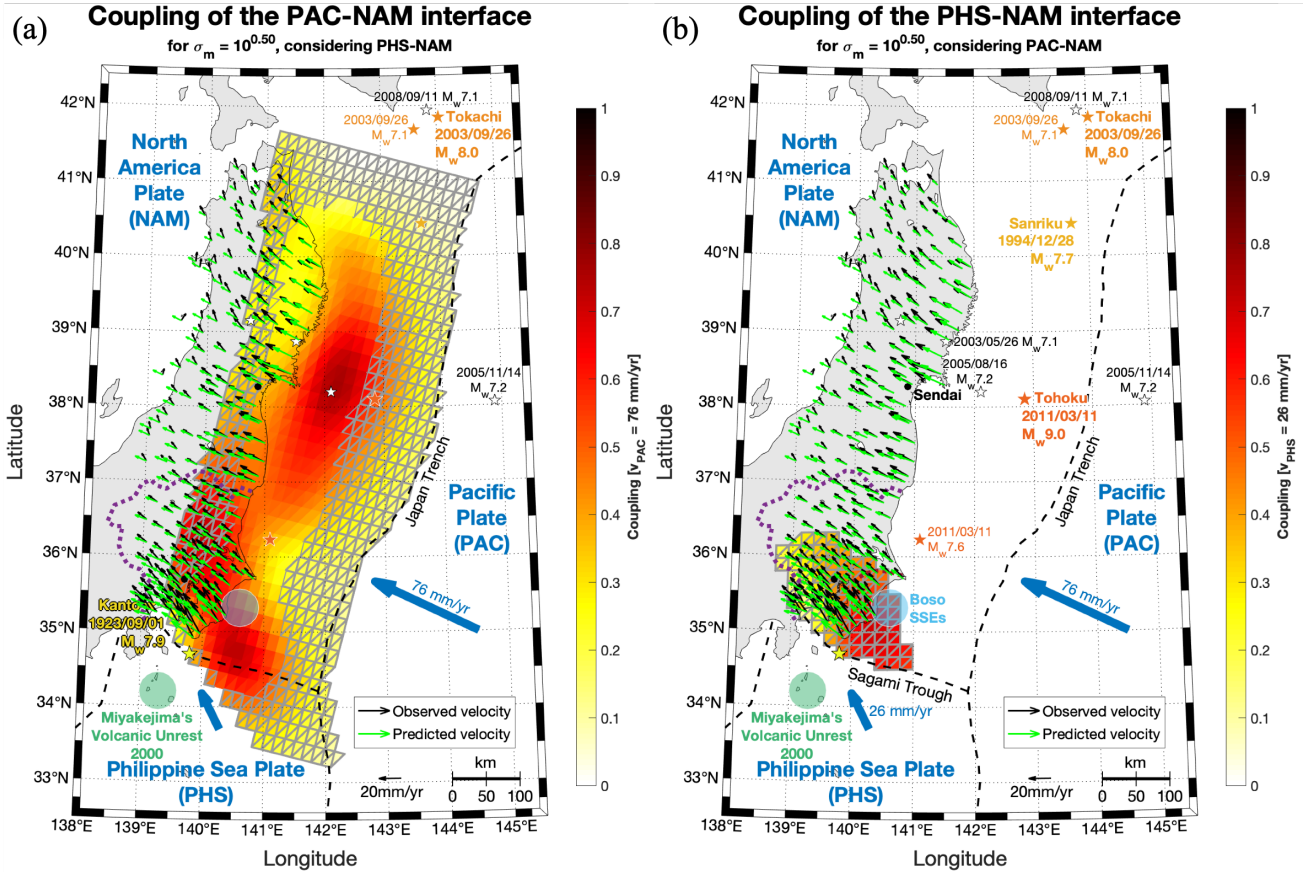

Figure S8. Coupling of the Pacific-North America (PAC-NAM) subduction interface (a) and the Philippine Sea-North America (PHS-NAM) subduction interface (b) for $\sigma_m = 10^{0.50}$. Same legend as Figure 4.

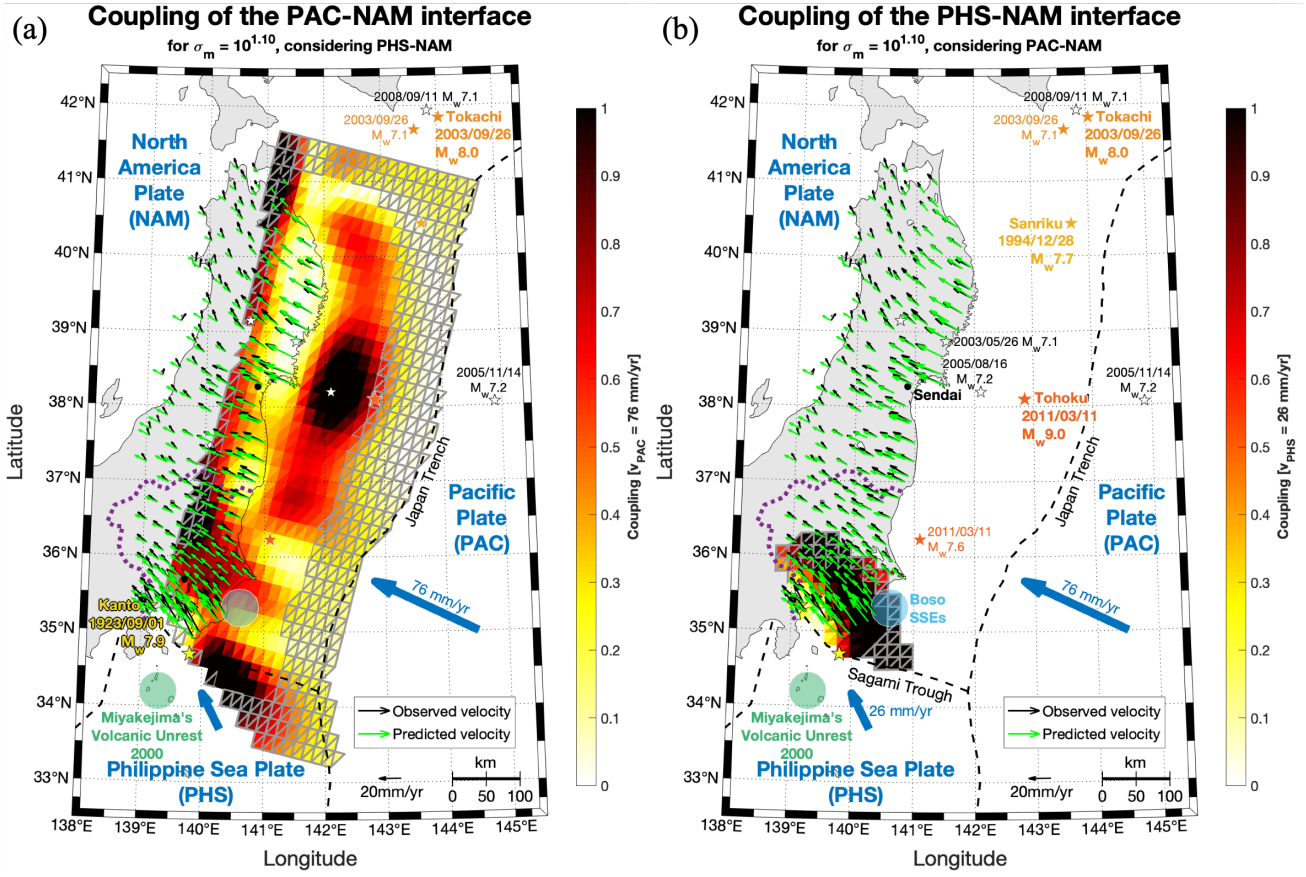

Figure S9. Coupling of the Pacific-North America (PAC-NAM) subduction interface (a) and the Philippine Sea-North America (PHS-NAM) subduction interface (b) for $\sigma_m = 10^{1.10}$. Same legend as in Figure 4.

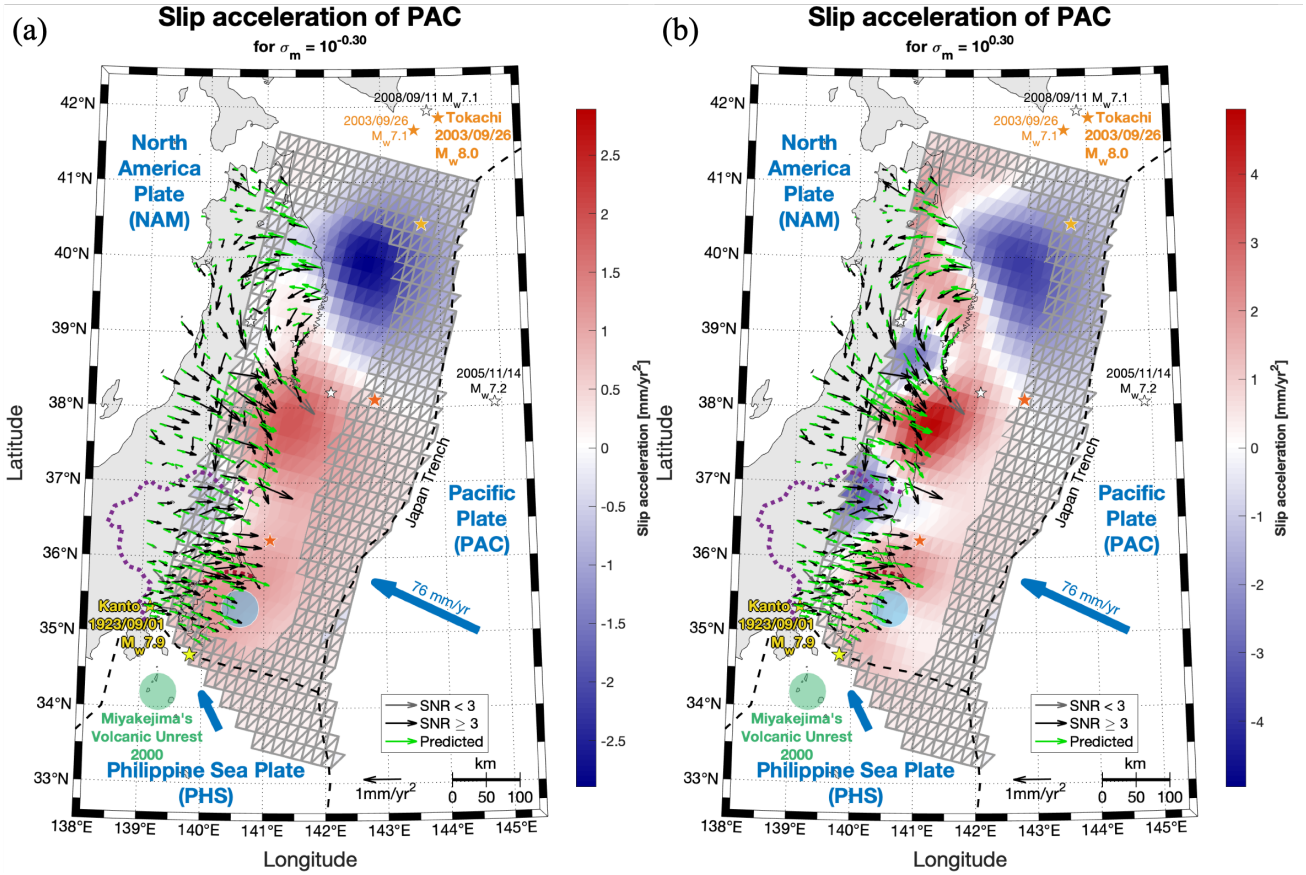

Figure S10. Slip acceleration of the Pacific (PAC) plate for $\sigma_m = 10^{-0.30}$ (a) and $\sigma_m = 10^{0.30}$ (b). Same legend as Figure 5. *Warning:* different colorbar scales!

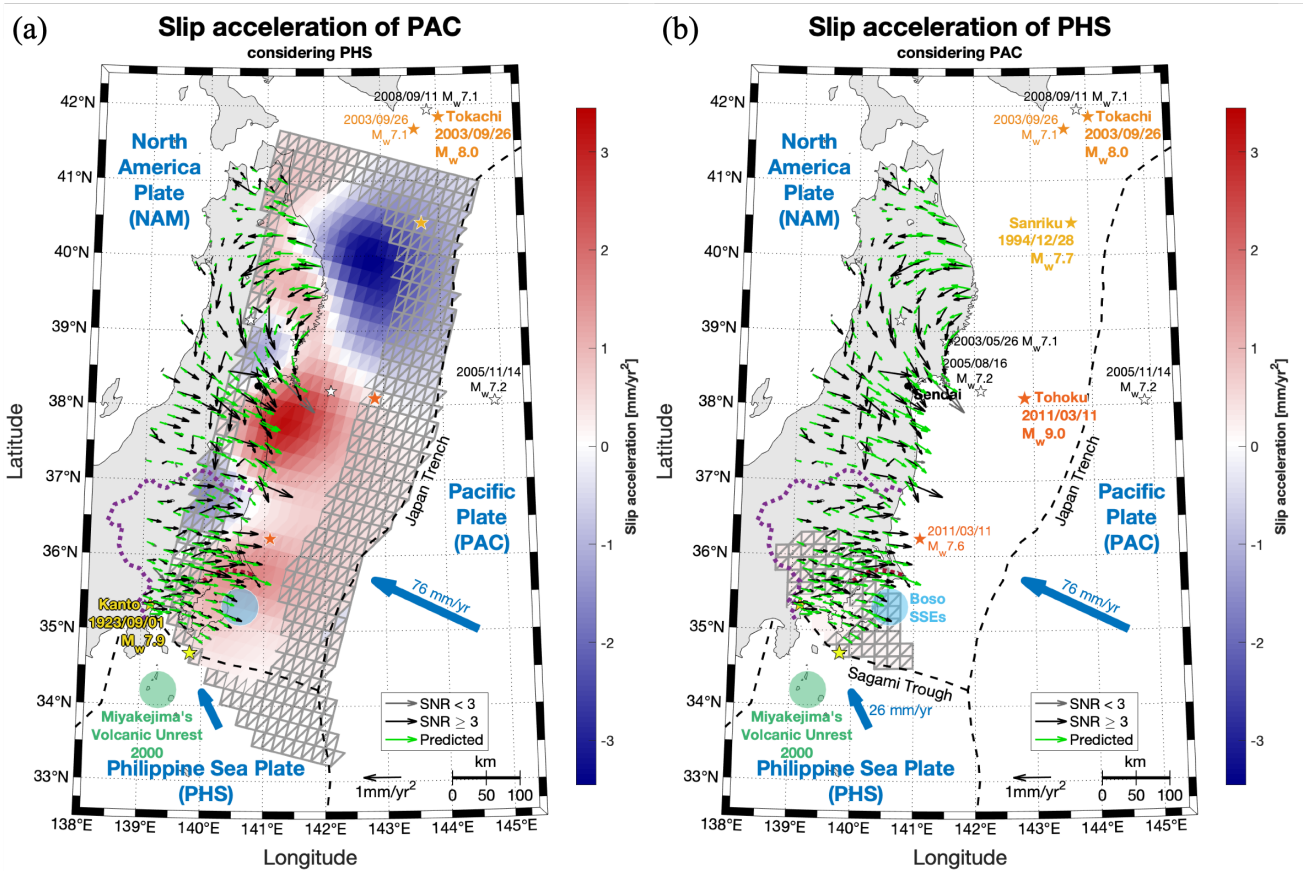

Figure S11. Slip acceleration of the Pacific (PAC) plate (a) and the Philippine Sea (PHS) plate (b) for the 2-plate inversion. Same legend as Figure 5.

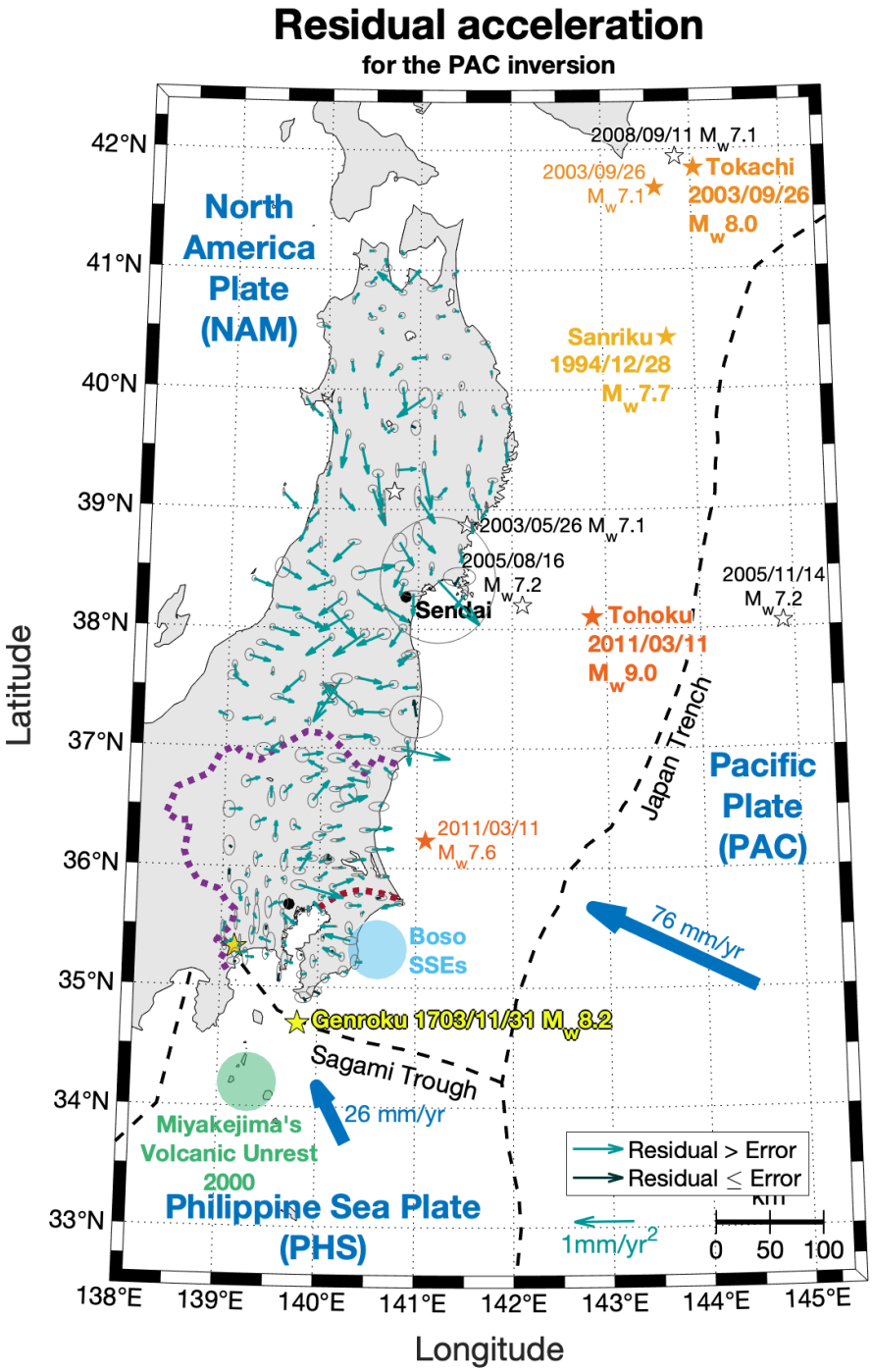

Figure S12. Residuals of the acceleration field inversion of the Pacific (PAC) plate. The error ellipse of the horizontal acceleration are shown for each station , as well as the residuals between the acceleration field (black, gray arrows in Figure 5) and the predicted surface acceleration (green arrows in Figure 5). The light arrows correspond to residuals higher than the acceleration error, and dark, to residuals small or equal to the acceleration error.

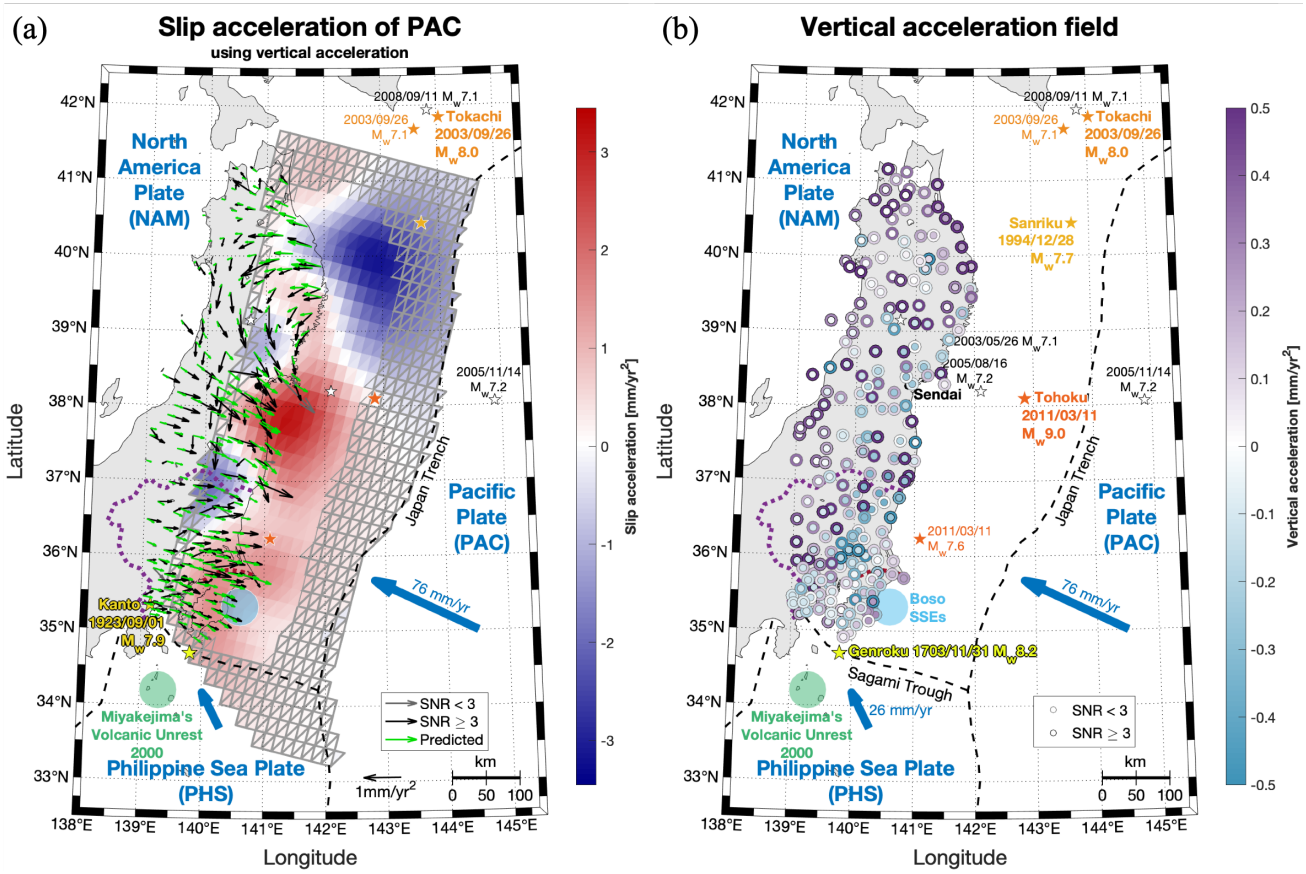

Figure S13. Slip acceleration of PAC accounting for vertical displacement. (a): Horizontal acceleration and slip acceleration; same legend as Figure 5. (b): Vertical acceleration; the outer circle represent the observed vertical acceleration while the inner circle represent the predictions. We distinguish the stations which have a signal-to-noise ratio greater than 3 (black contour), and those which fail to meet this criterion (grey contour, see Section 3.4); other elements are described in Figure 1.

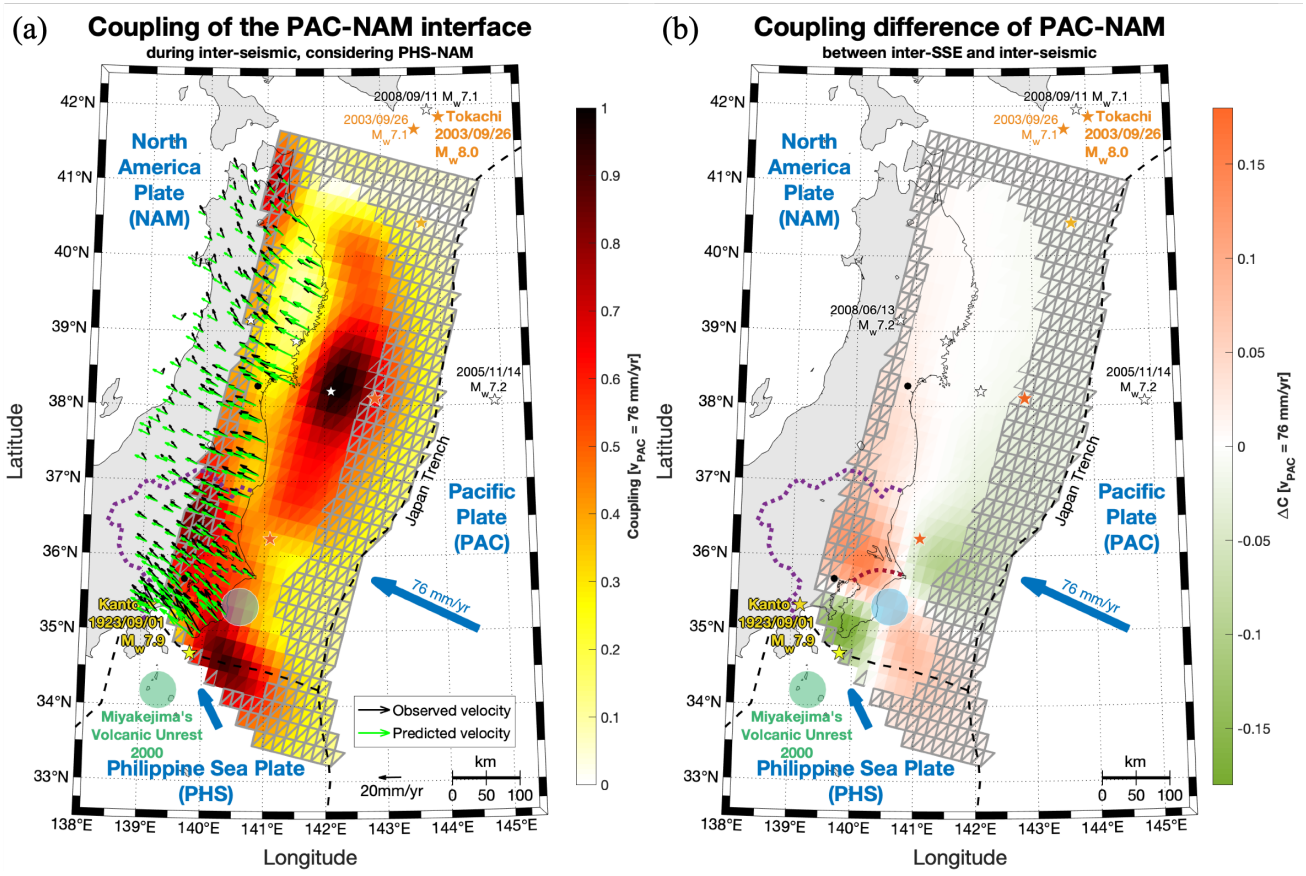

Figure S14. Impact of the Boso SSEs correction on the Pacific-North America (PAC-NAM) subduction interface coupling. (a): Inter-seismic coupling (for time series analysis without SSE modeling); same legend as Figure 4. (b): Coupling difference between inter-SSE coupling (Figure 4a) and inter-seismic coupling (a); orange: sub-fault more coupled with the Boso SSEs correction; green: sub-fault less coupled with the Boso SSEs correction; other elements are described in Figure 1.

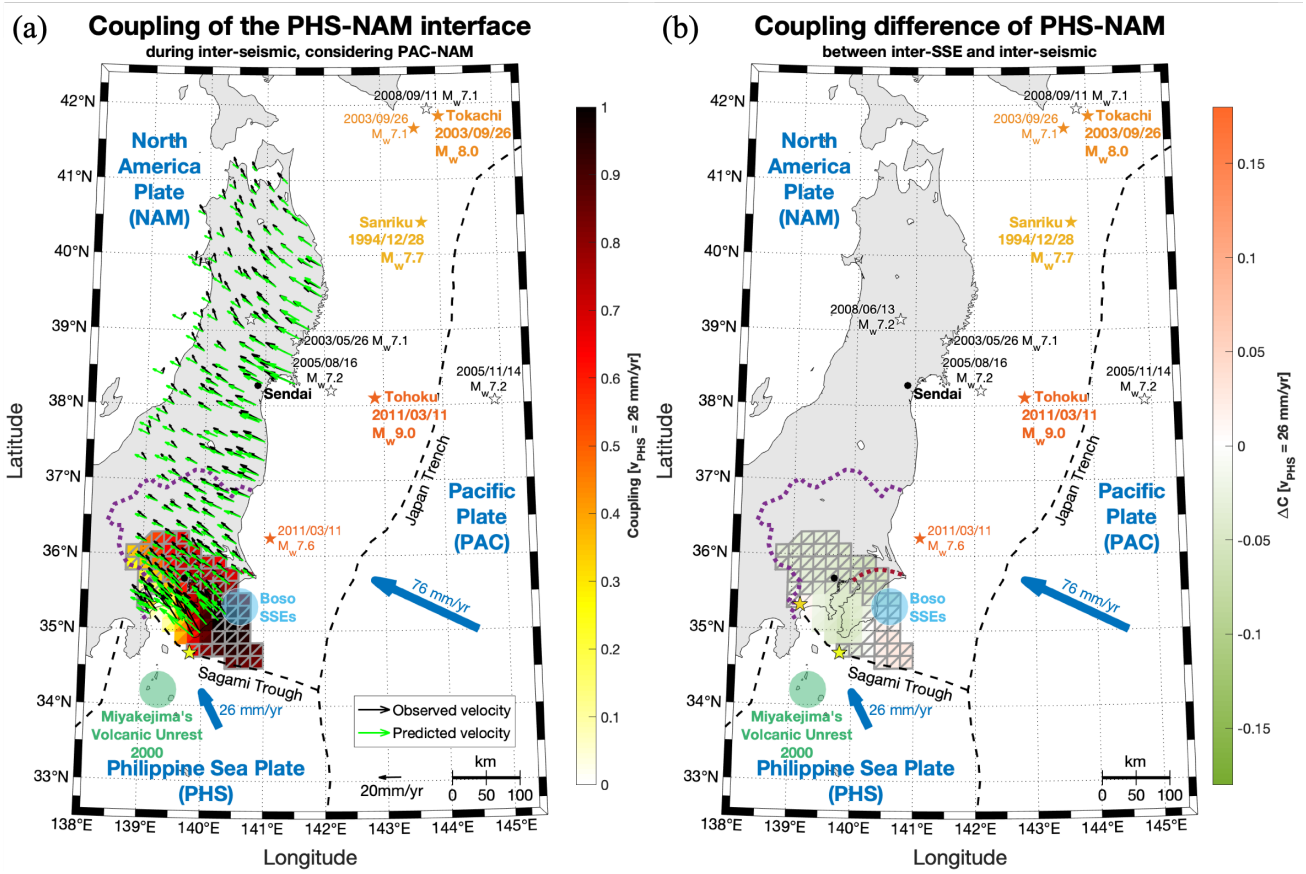

Figure S15. Impact of the Boso SSEs modelling on the Philippine Sea-North America (PHS-NAM) subduction interface coupling. (a): Inter-seismic coupling (for time series analysis without SSE modeling). (b): Coupling difference between inter-SSE coupling (Figure 4b) and inter-seismic coupling (a). Same legend as Figure S14.

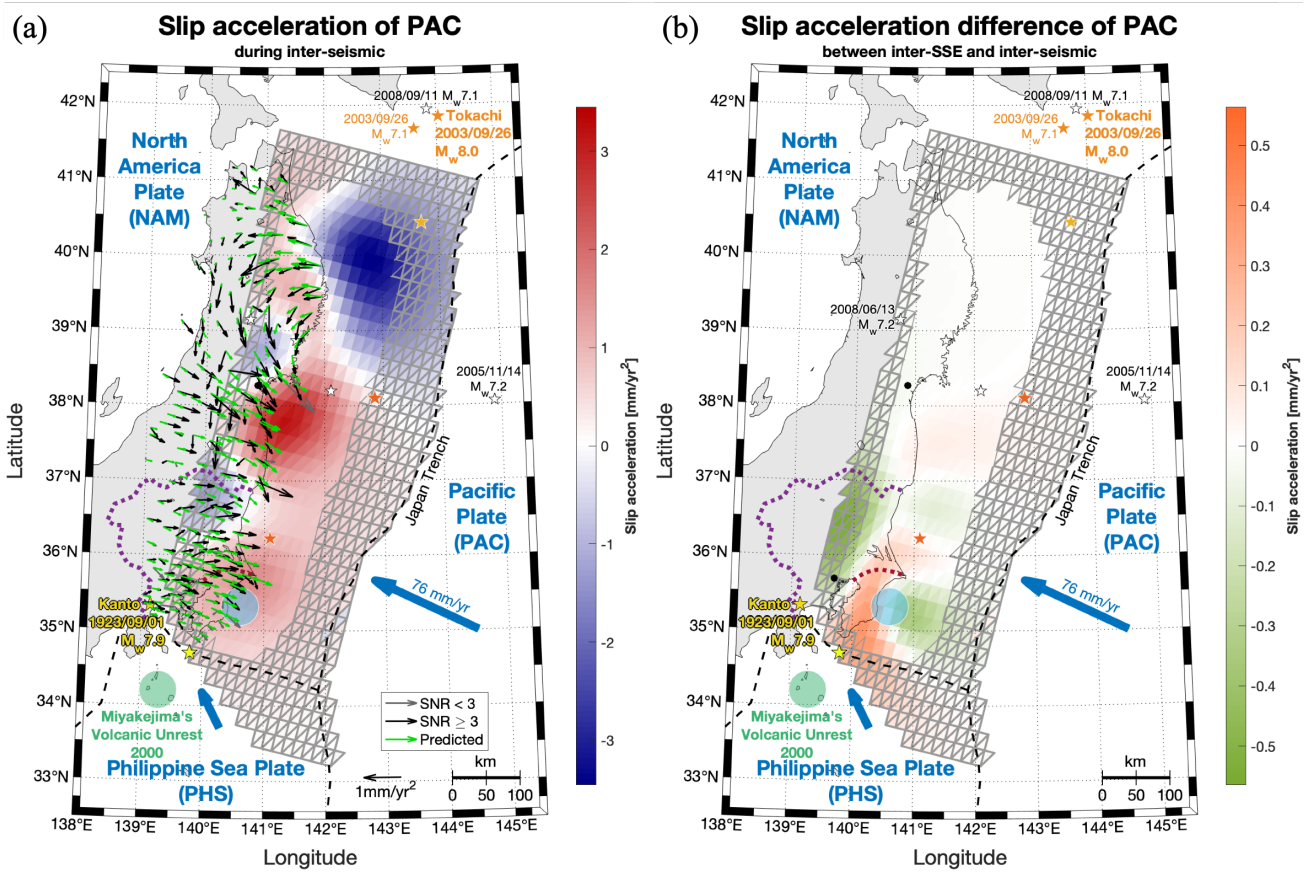

Figure S16. Impact of the Boso SSEs modelling on the Pacific (PAC) plate slip acceleration. (a): Inter-seismic slip acceleration (for time series analysis not modeling SSE); same legend as Figure 5. (b): Difference between the inter-SSE slip acceleration (Figure 5) and the inter-seismic slip acceleration (a).

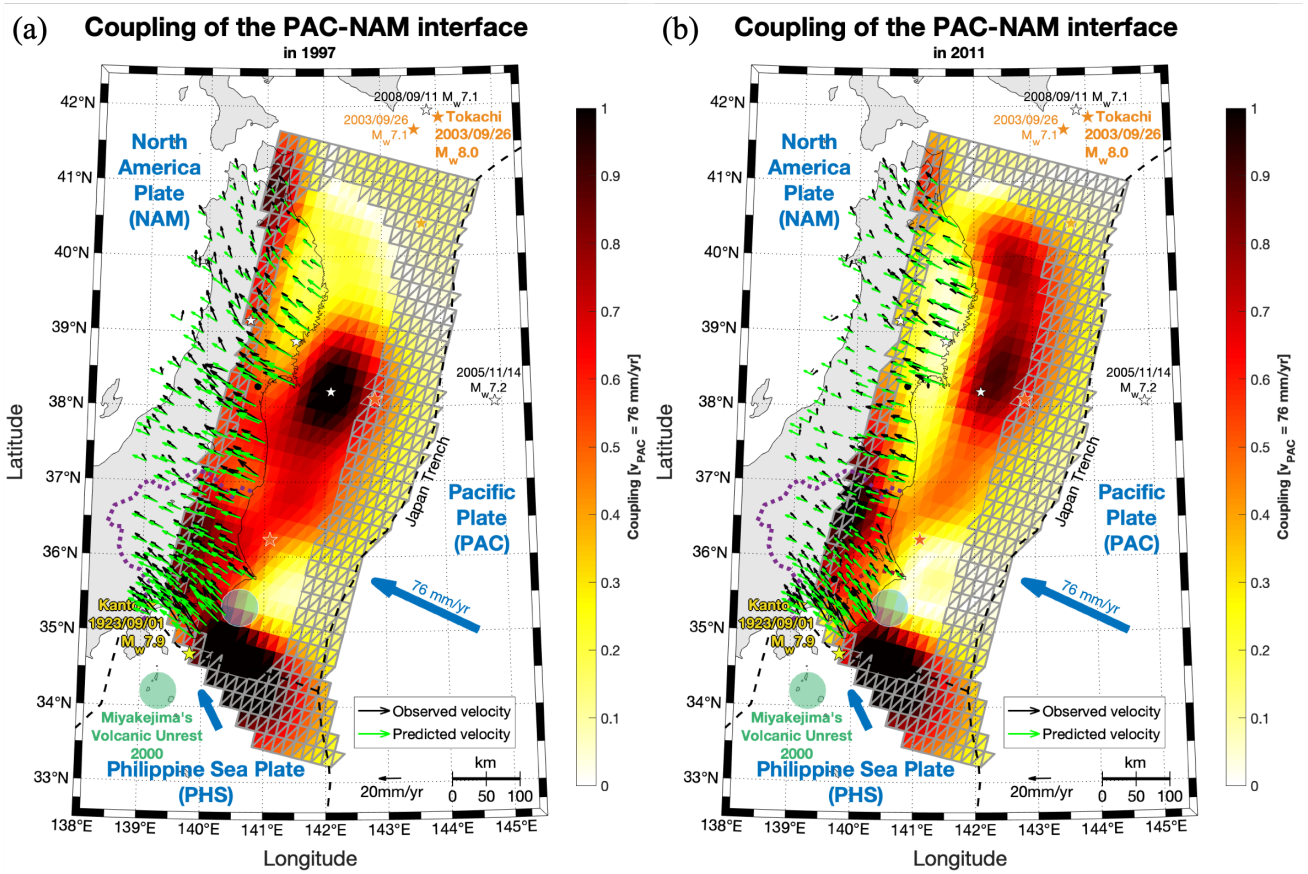

Figure S17. Coupling of the Pacific-North America (PAC-NAM) subduction interface in 1997 (a) and 2011 (b). Same legend as Figure 4.

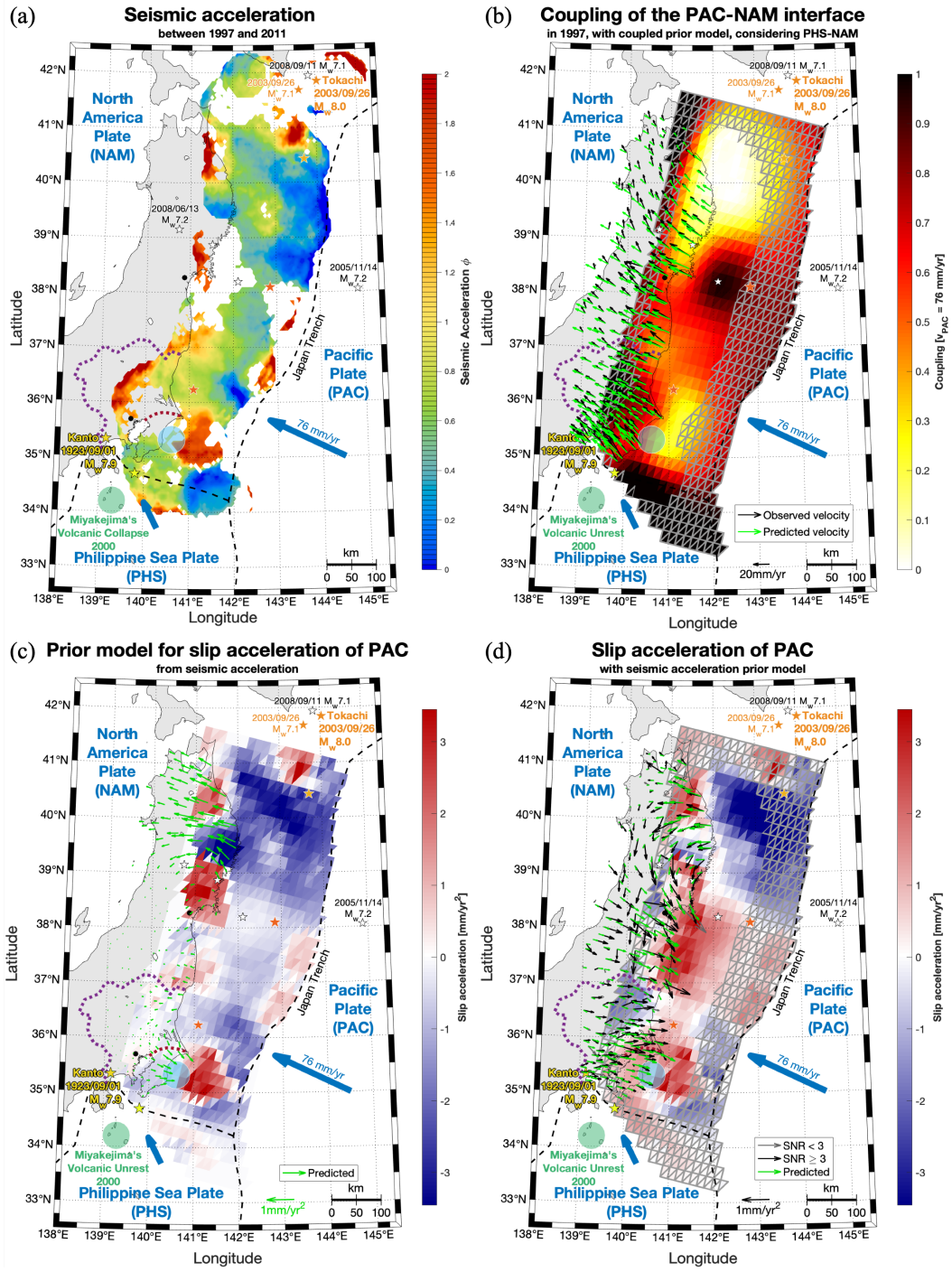

Figure S18. Seismic acceleration on the Pacific (PAC) plate between 1997 and 2011 as slip rate acceleration prior. (a): Seismic acceleration of the Pacific (PAC) plate between 1997 and 2011. (b) Coupling of the Pacific-North America (PAC-NAM) interface. (c): Prior slip acceleration model of the PAC plate based on the seismic acceleration (a) and the coupling (b) with Equation (18). (d): Slip acceleration of the PAC plate. Same legend as Figure 8.